Enhancement of calcium-dependent afterpotentials in oxytocin neurons of the rat supraoptic nucleus during lactation

Ryoichi Teruyama and William E. Armstrong

Department of Anatomy and Neurobiology, College of Medicine, University of Tennessee, Memphis, TN 38163, USA

The firing pattern of oxytocin (OT) hormone synthesizing neurons changes dramatically immediately before each milk ejection, when a brief burst of action potentials is discharged. OT neurons possess intrinsic currents that would modulate this burst. Our previous studies showed the amplitude of the Ca^{2+}-dependent afterhyperpolarization (AHP) following spike trains is significantly larger during lactation. In the present study we sought to determine which component of the AHP is enhanced, and whether the enhancement could be related to changes in whole-cell Ca^{2+} current or the Ca^{2+} transient in identified OT or vasopressin (VP) neurons during lactation. We confirmed, with whole-cell current-clamp recordings, our previous finding from sharp electrodes that the size of the AHP following spike trains increased in OT, but not VP neurons during lactation. We then determined that an apamin-sensitive medium-duration AHP (mAHP) and an apamin-insensitive slow AHP (sAHP) were specifically increased in OT neurons. Simultaneous Ca^{2+} imaging revealed that the peak change in somatic $[Ca^{2+}]_i$ was not altered in either cell type, but the slow decay of the Ca^{2+} transient was faster in both cell types during lactation. In voltage clamp, the whole-cell, Ca^{2+} current was slightly larger during lactation in OT cells only, but current density was unchanged when corrected for somatic hypertrophy. The currents, I_{mAHP} and I_{sAHP}, also were increased in OT neurons only, but only the apamin-sensitive I_{mAHP} showed an increase in current density after adjusting for somatic hypertrophy. These findings suggest a specific modulation (e.g. increased number) of the small-conductance Ca^{2+}-dependent K^+ (SK) channels, or their interaction with Ca^{2+}, underlies the increased mAHP/I_{mAHP} during lactation. This larger mAHP may be necessary to limit the explosive bursts during milk ejection.

(Received 7 March 2005; accepted after revision 3 May 2005; first published online 5 May 2005)
Corresponding author Ryoichi Teruyama: 855 Monroe Avenue, Department of Anatomy and Neurobiology, College of Medicine, University of Tennessee, Memphis, TN 38163, USA. Email: rteruyam@utmem.edu

The neurohypophysial hormones oxytocin (OT) and vasopressin (VP) are synthesized in the magnocellular cells (MNCs) located within the paraventricular (PVN) and the supraoptic nuclei (SON) of the hypothalamus. OT- and VP-containing vesicles travel from the sites of synthesis within the hypothalamic nuclei, by axoplasmic flow to axon terminals within the neurohypophysis where they are released into the general circulation in response to physiological demands. OT plays important roles in stimulating milk release and parturition, while VP produces antidiuretic and pressor effects during osmotic and cardiovascular challenge, respectively (Poulain & Wakerley, 1982).

The release of OT and VP is a function of the rate and pattern of neuronal activity of SON and PVN neurons (Poulain & Wakerley, 1982). During lactation, OT neurons display a short (2–4 s), high-frequency (up to 80 Hz) burst of action potentials preceding each milk ejection. This bursting activity is synchronized among all OT neurons (Belin *et al.* 1984), and results in a bolus release of OT into the bloodstream, necessary for uterine contraction or contraction of myoepithelial cells in the mammary glands. This pulsatility is believed to maximize the biological effects of OT and allows the neurons to recover from secretory fatigue (Bicknell, 1988).

Coincident with the physiological demands, OT neurons undergo considerable plasticity in their morphological (Hatton, 1990; Theodosis & Poulain, 1993) and physiological properties (Teruyama & Armstrong, 2002*a*) during pregnancy and lactation. There are increases in both GABAergic (Gies & Theodosis, 1994; Brussaard *et al.* 1999) and glutamatergic (El Majdoubi

 DOI: 10.1113/jphysiol.2005.085985

et al. 1996; Stern *et al.* 2000) synaptic activity. Changes in the intrinsic properties specific to OT neurons include an increase in the amplitude of the Ca^{2+}-dependent afterhyperpolarization (AHP), and a higher incidence of neurons expressing the Ca^{2+}-dependent depolarizing after potential (DAP) (Stern & Armstrong, 1996; Teruyama & Armstrong, 2002*a*). These changes, which occur during late pregnancy (Teruyama & Armstrong, 2002*a*), indicate that OT neurons transform their intrinsic properties prior to their increased activity during parturition and suckling.

Among MNCs, there are at least three AHP components following a train of action potentials. The fast AHP (fAHP) immediately follows spike repolarization and derives from probable mixtures of Ca^{2+}-dependent K^+ currents (Stern & Armstrong, 1997; Dopico *et al.* 1999), and other high-voltage-gated K^+ currents (Bourque, 1988; Shevchenko *et al.* 2004). The medium AHP (mAHP) has a duration of 200–500 ms and is blocked by apamin or tubocurarine (Stern & Armstrong, 1997; Greffrath *et al.* 1998; Teruyama & Armstrong, 2002*a*), suggesting the involvement of the Ca^{2+}-activated small-conductance K^+ (SK) channels. The third, slowest component (sAHP) appears with a longer spike train (Greffrath *et al.* 1998), and is inhibited by muscarine (Ghamari-Langroudi & Bourque, 2004). Although the AHP modulated during pregnancy and lactation (Stern & Armstrong, 1996; Teruyama & Armstrong, 2002*a*) is kinetically related to the mAHP, its identity has not been confirmed.

The present study was conducted to identify the currents underlying the AHPs in OT neurons that are altered during lactation, and to determine whether any changes in these Ca^{2+}-dependent events could be related to changes in the whole-cell Ca^{2+} current or in the spike-associated $[Ca^{2+}]_i$ transient. The results have been published previously in abstract form (Teruyama & Armstrong, 2002b, 2004).

Methods

Animals and slice preparation

Brain slices containing the SON were prepared from virgin adult (180–210 g body weight; random cycling) and lactating (8–12 days of lactation) rats (Sprague-Dawley, Harlan Laboratories, Indianapolis). The rats were deeply anaesthetized with sodium pentobarbital (50 mg kg^{-1}, I.P.) and perfused through the heart with an artificial cerebrospinal fluid (ACSF) solution (see below) in which NaCl was replaced by an equiosmolar amount of sucrose. Their brains were removed and sliced in the coronal plane at a thickness of 250 μm in ice cold ACSF. Slices were maintained in an ACSF, which was bubbled continuously with 95% O_2–5% CO_2, containing (mM): 124 NaCl, 3 KCl, 2.0 $CaCl_2$, 1.3 $MgCl_2$, 1.24 NaH_2PO_4, 25 $NaHCO_3$, 0.2 ascorbic acid, and 10 D-glucose (pH 7.4) Slices were stored at room temperature prior to recording.

Voltage clamp

Whole-cell voltage-clamp recordings were obtained either with Axon 200B or 700 A amplifiers (Axon Instruments, Foster City, CA, USA). Traces were acquired digitally at 20 kHz and filtered at 5 kHz with Digidata 1320 A or 1322 A (Axon Instruments, Union City, CA) in conjunction with pClamp 8 software (Axon Instruments). Whole-cell capacitance and series resistance were compensated 75–80%. Quantitative estimates of whole-cell capacitance were obtained by fitting the current decay evoked with a +5 mV, 10 ms step. The patch solution for analysing AHP tail currents consisted of (mM): 135 $KMeSO_4$, 8 KCl, 1 $MgCl_2$, 10 Hepes, 0.2 EGTA, 0.4 GTP(Na), 2 ATP(Mg). For recording of AHP tail currents, 5 mM CsCl was added to ACSF to suppress the DAP (Ghamari-Langroudi & Bourque, 1998). In some cases, 100 nM apamin (Sigma, St. Louis, MO, USA) or 400 μM $CdCl_2$ was added to ACSF.

The patch solution for analysing Ca^{2+} currents consisted of (mM): 180 *N*-methyl-D-glucamine, 4 $MgCl_2$, 40 Hepes, 10 EGTA, 12 phosphocreatine, 0.4 GTP (Na), 2 ATP (Mg). Ca^{2+} currents were isolated by switching ACSF to a medium consisting of: (mM): 110 NaCl, 2 TEA-Cl, 10 CsCl, 1 $MgCl_2$, 10 Hepes, 4 $CaCl_2$, 10 glucose, 0.0005 TTX, 0.1 picrotoxin.

Intracellular solutions were adjusted to a pH of 7.3 with KOH, and contained 0.20% biocytin (Sigma) to identify the patched cell (see Immunocytochemistry below). The liquid junction potentials were approximately −10 mV and −5 mV with the $KMeSO_4$ and the *N*-methyl-D-glucamine patch solutions used, respectively. The data presented were not corrected for junction potentials. The currents obtained were an average of five runs through a particular trial. All media were saturated with 95% O_2–5% CO_2, with a pH of 7.3–7.4, had an osmolality of 290–300 mOsmol (kg $H_2O)^{-1}$, and were warmed to 33°C during the recording.

Simultaneous current clamp and Ca^{2+} fluorescence imaging

Simultaneous whole-cell current-clamp and Ca^{2+} fluorescence imaging records were acquired using an Axopatch 200B (Axon Instruments) amplifier and a cooled CCD camera (Sensicam: PCO, Kellheim, Germany) in combination with a single Windows platform PC running software written by Dr J. C. Callaway, based on software developed by Lasser-Ross *et al.* (1991). Recordings were taken using borosilicate electrodes (4–8 MΩ resistance) filled with a solution containing (mM): 135 $KMeSO_4$,

8 KCl, 1 $MgCl_2$, 10 Hepes, 2 adenosine5′-triphosphate (ATP), and 0.4 guanosine 5′-triphosphate (GTP), 0.1 fura-2 (penta K^+ salt: Molecular Probes). The intracellular solution also contained 0.2% biocytin (Sigma) to identify the patched cell (see Immunocytochemistry below). Current-clamp recordings were digitized at 16-bit resolution at 10 kHz. Optical data were acquired using the Imago Sensicam (T.I.L.L. Photonics, Planegg, Germany). To obtain optical data, the fura-2 were excited at a wavelength of 380 nm using a USHIO UXL-150MO 150 W xenon arc lamp, and fluorescence changes was measured at an emission wavelength of 520 ± 40 nm (filters from Chroma Technology, Brattleboro, VT, USA). The frame rate was 40 Hz with pixels binned (4×4) at run time. Photobleaching was corrected by subtracting the Ca^{2+} signal from an equal-length control sweep containing no stimulus at a hyperpolarized holding potential (−70 mV), at which no Ca^{2+} entry could be detected. Fluorescence was corrected further for tissue autofluorescence by subtracting the background fluorescence near the filled cell. Measurements were made from the soma, specifically avoiding the brighter cell nucleus when visible. More detailed information can be obtained elsewhere (Roper *et al.* 2003).

Immunocytochemistry

Following recording, the slices were fixed with 4% paraformaldehyde and 0.2% picric acid in phosphate buffered saline (PBS) at 4°C overnight, and processed for double-immunofluorescence labelling according to previously published procedures (Teruyama & Armstrong, 2002*a*). The anti-VP-neurophysin antiserum is a rabbit polyclonal provided by Alan Robinson (retired), and was used at a 1 : 20 000 dilution. The anti-OT-neurophysin antibody (PS36) is a mouse monoclonal antibody provided by Harold Gainer (National Institutes of Health), and was used at a 1 : 500 dilution. All antibodies and other labelling reagents were dissolved in PBS containing 0.5% Triton X-100. The slices were incubated for 48–72 h at 4°C, followed by the incubation in a cocktail of secondary antibodies and avidin-AMCA (7-amino-4-methylcoumarin-3-acetic acid; Vector Laboratories, Burlingame, CA, USA) overnight at 4°C. The secondary antibodies used were fluorescein isothiocyanate (FITC)-conjugated goat anti-rabbit and Texas Red-conjugated goat antimouse immunoglobulin G (IgG). Avidin-AMCA was used to visualize the recorded cells. Neurons were considered as either OT or VP types only if positive staining of one antibody was complemented by a negative reaction with the other (Fig. 1). In the few cases where the intracellularly filled neuron was located deeper than the antibodies penetrated, the slice was cryoprotected with 50% glycerol in PBS, further sectioned at 40 μm, and the procedure repeated.

Results

Current clamp and Ca^{2+} fluorescence imaging

Prominent AHPs were observed following the train of action potentials in all the SON neurons examined. The peak amplitudes of the AHP were reached by 15–20 spikes in OT neurons from virgin rats (Fig. 2). Since AHP amplitude is dependent upon the number of spikes during the train (Andrew & Dudek, 1984; Bourque *et al.* 1985; Kirkpatrick & Bourque, 1996), we gave a fixed number of 20 spikes evoked by 5 ms current injections at 20 Hz to generate AHPs and make equitable comparisons across states.

We also used simultaneous Ca^{2+} imaging to obtain the amplitude and decay of spike-evoked Ca^{2+} transients associated with AHPs (Fig. 3). The relative change in fura-2 fluorescence ($\Delta F/F$) is closely proportional to $[Ca^{2+}]_i$ for changes in $\Delta F/F$ of ≤ 0.5 (Lev-Ram *et al.* 1992). Since the peaks of $\Delta F/F$ values from the neurons recorded were less than 0.5, we use the $\Delta F/F$ value for the relative changes

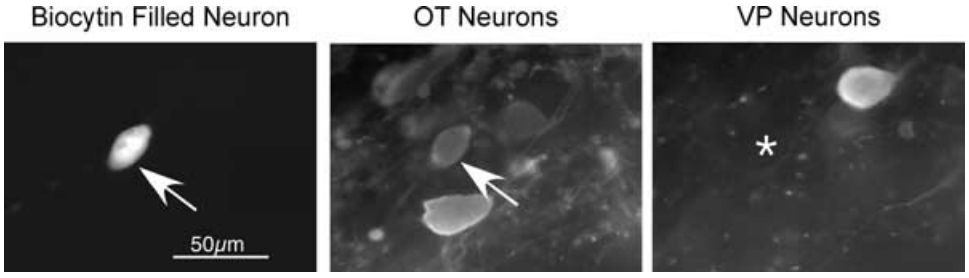

Figure 1. Immunocytochemically classified OT neuron
The injected cell was visualized by AMCA conjugated avidin (arrow, left panel). The tissue was then labelled for OT- and VP-neurophysins (NP) by double immunofluorescence using Texas red dye-conjugated and fluorescein isothiocyanate-conjugated secondary antibodies, respectively. The recorded cell was immunoreactive to OT-NP (arrow, middle panel), but not to VP-NP (asterisk, right panel).

in $[Ca^{2+}]_i$. For convenience, we have plotted $\Delta F/F$ as a percentage. A rapid rise in somatic $\Delta F/F$ was observed during the trains of 20 spikes at 20 Hz, and decayed with a time constant of 2–4 s from the end of the spike train (Fig. 3*C*). An additional faster component in the decay was observed in 5 out of 13 OT neurons from lactating rats, 7 out of 13 OT neurons from virgin rats, 2 out of 10 VP neurons from lactating rats, and 5 out of 9 VP neurons from virgin rats.

To investigate which AHPs were specifically altered during lactation, the bee venom apamin that blocks the mAHP in MNCs (Bourque & Brown, 1987; Armstrong *et al.* 1994; Greffrath *et al.* 1998) was employed. First, AHPs were obtained in the presence of 5 mM Cs^+ in order to block the time-overlapping DAP (Ghamari-Langroudi & Bourque, 1998). Bath application of 5 mM Cs^+ produced a deceleration of the decay of the AHPs and revealed the presence of an sAHP in addition to the mAHPs (Fig. 3*D*). Subsequent application of 100 nM apamin blocked the mAHP and left a slowly decaying sAHP in all MNCs examined (Fig. 3*E*). However, Cs^+ or apamin had no effect on the properties of the Ca^{2+} transient in MNCs, regardless of cell type or the reproductive state of animal (Fig. 3*D* and *E*).

The effects of lactation on the AHP and the calcium transient during the AHPs were assessed first before an application of apamin (Fig. 4). The peak amplitude of the AHP significantly increased in OT neurons from lactating animals, but not in VP neurons (Fig. 4*A* and *B*), whereas peak $\Delta F/F$ did not change significantly during lactation in either cell type (Fig. 4*A* and *C*). However, the decay time constant of the Ca^{2+} transient became significantly shorter during lactation in both cell types (Fig. 4*A* and *D*).

Subsequently, the apamin-sensitive mAHP was isolated by the subtraction of apamin traces from controls (Fig. 5*A*). The peak amplitude and area of the apamin-sensitive mAHP were significantly enhanced during lactation among OT neurons, but not among VP neurons (Fig. 5*B* and *C*). The decay of the isolated mAHP was mono-exponential, and the time constant of the decay remained constant during lactation in both cell types (Fig. 5*D*). The residual AHP following apamin represents the sAHP. The average area and the peak amplitude of the sAHP in OT neurons from lactating animals were significantly larger than those from virgins, while no differences were found among VP neurons (Fig. 6*A* and *B*). The area rather than the time course was used to quantify the sAHP, as its shape varied among cells, and could not typically be described with a single exponential. In addition, the sAHP appeared different between OT and VP neurons, peaking later in VP than in OT neurons (Fig. 6*A*). These results suggest that both the mAHP and sAHP were specifically augmented among OT neurons in response to lactation, but this change was not related to an increased bulk Ca^{2+} response in the soma.

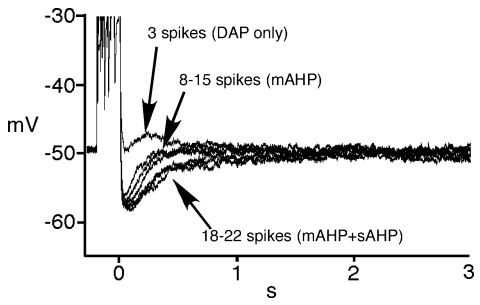

Figure 2. Example of relationships between number of spikes and the afterpotentials
The traces were obtained in a OT neuron from a virgin rat. Three spikes during 200 ms current injection evoked DAP, indicating AHPs are still not fully activated. When increasing the depolarizing current, the mAHP (most likely apamin sensitive) reached a peak after 8–15 spikes. An abrupt deceleration of the decay of the AHP is observed after 18–22 spikes, indicating the sAHP was activated.

Whole-cell Ca^{2+} currents

Since SON neurons in the slice exhibit varying degrees of dendritic arborization, poor space clamp was sometimes evident in voltage-clamp recordings of Ca^{2+} currents. This was indicated by the abrupt changes in the current during equally spaced voltage steps, broad tail currents, a skewed current–voltage (I–V) relationship, and an escaping tail current. While use of dissociated cells would be indicated to avoid this problem, we have not been able to routinely identify cell types with this technique, while we can routinely identify OT and VP neurons on slices by immunocytochemistry. Furthermore, dissociation requires enzymatic treatments that might make a comparison with our previous experiments difficult. For these reasons we measured Ca^{2+} current using rat brain slices, excluding neurons exhibiting obvious poor space clamp (8/20 in OT neurons from virgin rats, 3/13 OT neurons from lactating rats, 3/11 VP neurons from virgin rats, 5/17 VP neurons from lactating rats were excluded). We did not analyse the fast kinetic properties of these currents, which are more likely to be influenced by spatially distributed channels.

Voltage-dependent Ca^{2+} currents were obtained from the immunoidentified OT and VP neurons from the SON in brain slices from virgin and lactating rats. Depolarizing voltage steps (200 ms) from −90 mV elicited inward currents that were characterized by an initial transient peak, followed by a sustained portion over the 200 ms pulse (Fig. 7*A*). These inward currents were blocked by 400 μM Cd^{2+} (Fig. 7*B*). The I–V relationships revealed that the currents were activated at potentials more depolarized than −50 mV, peaked between −10 and 0 mV, and had reversal potentials of about +50 mV (Fig. 7*C*).

The *I–V* relationships measured at the peak and sustained regions were similar. The sustained and peak Ca^{2+} current obtained from steps increased significantly in OT, but not VP neurons during lactation (Fig. 7*D*). The whole-cell capacitance also increased significantly during lactation in OT, but not VP neurons (Fig. 7*E*). When the currents were adjusted for cell membrane capacitance, the difference in Ca^{2+} current density was not significant in either cell type (Fig. 7*F*). These data suggest that somatic Ca^{2+} channel density is probably not increased during lactation,

Voltage clamp of I_{AHP}

The currents underlying the mAHP (I_{mAHP}) and sAHP (I_{sAHP}) were examined in voltage clamp to determine whether they were altered during lactation. Outward tail currents were evoked by a depolarizing voltage command step (200 ms) to +10 mV, from a holding potential of −70 mV in the presence of 5 mM Cs^+, which was used to block DAP (Ghamari-Langroudi & Bourque, 1998). The outward current had an initial transient

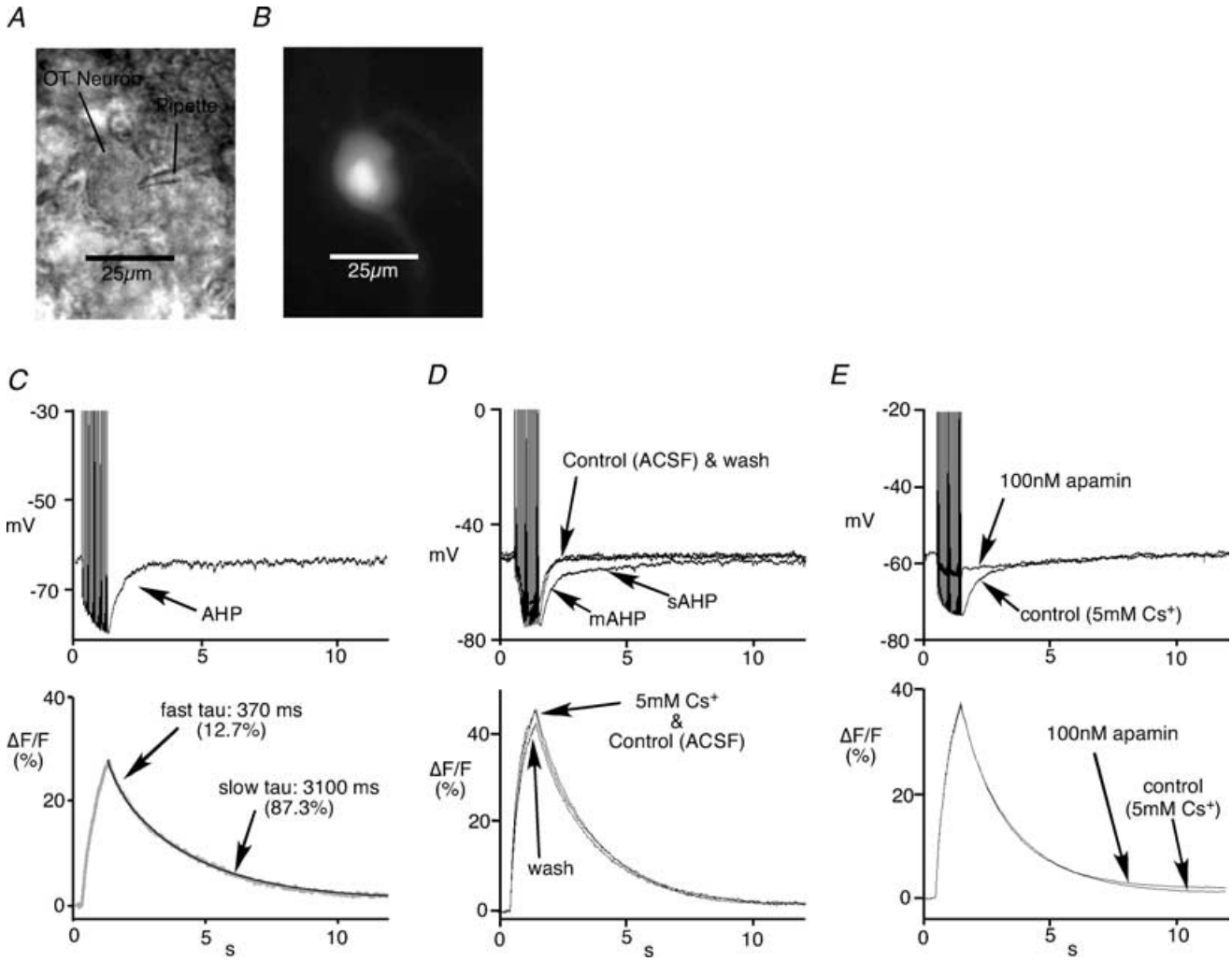

Figure 3. Simultaneous current clamp and Ca^{2+} imaging
A, a photomicrograph of a pipette-patched OT neuron from the SON. *B*, Fura-2 image of the OT neuron showing a location in the soma where Ca^{2+} fluorescence data were measured. The brightest area is the nucleus. Nuclei were not measured. *C*, an example of simultaneous recording of current clamp and Ca^{2+} fluorescence imaging. An accumulation of Ca^{2+} was observed during the train of spikes, followed by slow decay. This neuron had a faster component in the decay of the Ca^{2+} transient in addition to the slow component. The faster component was determined, if its amplitude coefficient exceeded 10% of the total coefficients. Tau, time constant. *D*, an example of the effect of 5 mM Cs^+ on the AHP and Ca^{2+} transient in an OT neuron. The bath application of 5 mM Cs^+ resulted in abrupt deceleration of the decay of the AHPs, and therefore revealed the presence of the sAHP. The effect was reversed by washing of the brain slice with normal ACSF. However, the Ca^{2+} transient was not affected by the application of Cs^+. *E*, an application of 100 nM apamin blocks mAHP, but has no effect on the Ca^{2+} transient.

component (I_{fAHP}), though this was not our interest. The outward currents following the I_{fAHP} decayed as a double exponential, with one time constant similar to that of the mAHP and the second time constant similar to that of the sAHP. Apamin (100 nM) blocked I_{mAHP} but not I_{sAHP} (Fig. 8*A*). I_{mAHP} was isolated by subtracting traces in the presence of apamin from control traces (Fig. 8*B* and *C*). The average peak amplitude of I_{mAHP} in OT neurons was larger during lactation, with no change in VP neurons (Fig. 8*D*). The whole-cell capacitance also increased significantly during lactation in OT neurons, indicating the expected hypertrophy, but not in VP neurons (Fig. 8*E*). When the peak amplitude of I_{mAHP} was adjusted for this increased capacitance, I_{mAHP} density was increased significantly only in OT neurons during lactation (Fig. 8*F*). The decay time constant of the I_{mAHP} did not change significantly (Fig. 8*G*).

The residual long tail current after the application of apamin represented I_{sAHP}. This I_{sAHP} was well fitted by a single exponential curve (Fig. 9*A* and *B*). To avoid contaminating the data with the I_{fAHP}, all fits to I_{sAHP} decay began at 1 s after the end of square pulse, where its amplitude was measured as an index of I_{sAHP} amplitude. The time constant of the decay was ~3.5 s and very similar to the decay from the sAHP, and did not change in response to lactation regardless of cell type (Fig. 9*C*). The amplitude of I_{sAHP} showed a small but significant increase in OT neurons during lactation (Fig. 9*D*). However, when adjusted by the cell membrane capacitance, the apparent I_{sAHP} density was unchanged. (Fig. 9*E*)

Discussion

During milk ejection, OT neurons exhibit brief (~4 s) explosive bursts followed by a transient decrease in tonic firing. The intrinsic properties of OT neurons would shape this burst, and our previous studies with sharp electrode recordings have shown marked changes in spike afterpotentials during lactation (Stern & Armstrong, 1996; Teruyama & Armstrong, 2002*a*). In the present study, changes in AHPs were confirmed with whole-cell recordings, and we demonstrate that these changes are primarily the result of OT neuron-specific changes

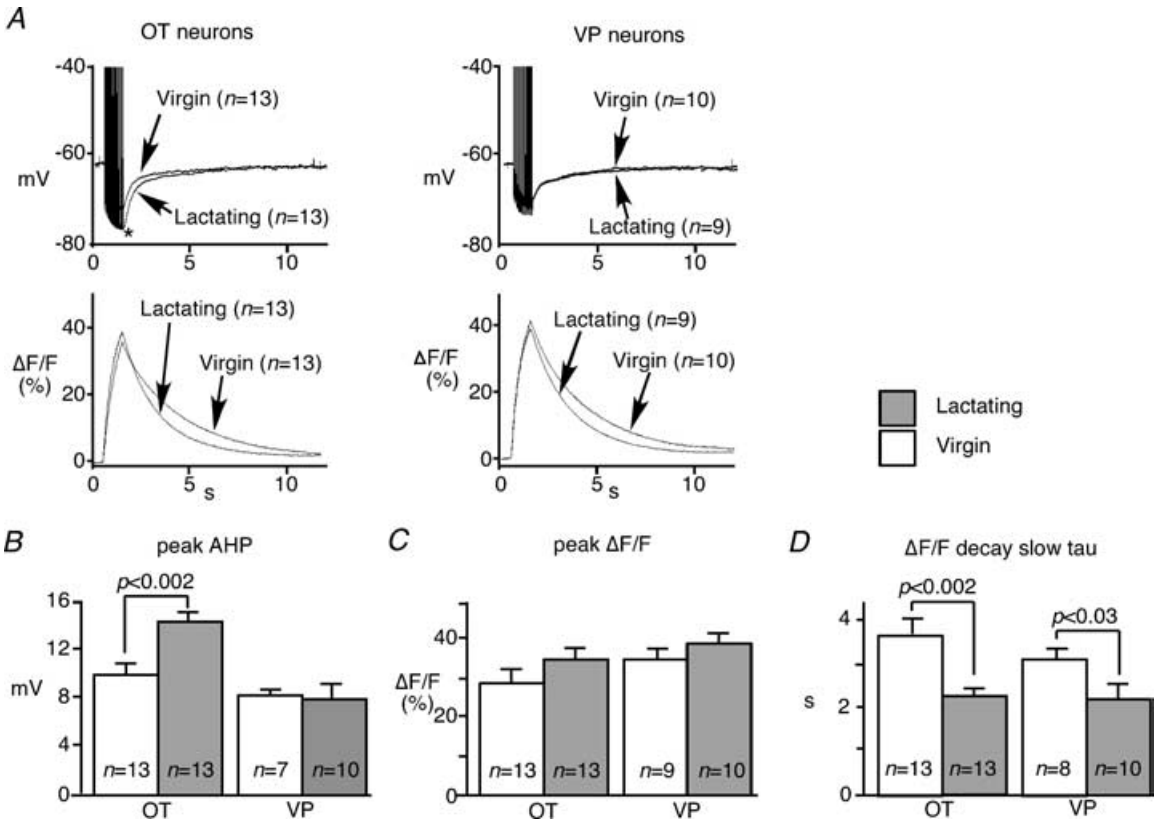

Figure 4. AHPs and Ca^{2+} transients during lactation
A, averaged AHPs and calcium transients from recorded neurons in the presence of 5 mM Cs^+ for comparison between lactating and virgin rats. *B*, the peak amplitude of AHP was significantly larger in OT neurons during lactation, while such alteration was not observed among VP neurons. C, the peak $\Delta F/F$ amplitude did not increase significantly. *D*, the slow time constant of $\Delta F/F$ became significantly faster during lactation in both OT and VP neurons.

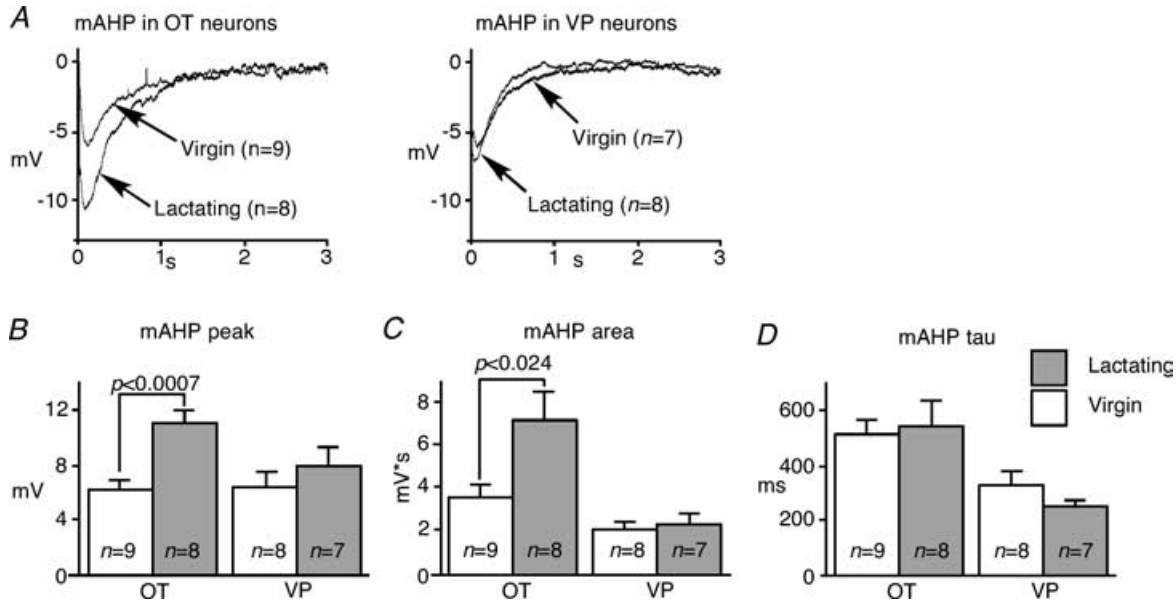

Figure 5. The apamin-sensitive mAHP increases during lactation
A, the mathematically isolated apamin-sensitive mAHP in OT and VP neurons from virgin and lactating animals. The traces are averaged from all cells. *B* and *C*, the peak amplitude and area of mAHP are enhanced during lactation in OT neurons, but not in VP neurons. *D*, the time constant (tau) of the mAHP decay did not change in either cell type.

in an apamin-sensitive current, I_{mAHP}, with a smaller contribution from a slower component, I_{sAHP}.

mAHP

In many neurons an apamin-sensitive mAHP results from small conductance Ca^{2+}-dependent K^+ (SK) channels (Bond *et al.* 1999). Four genes comprise the SK channel gene family, and three of them: *SK1*; *SK2*; and *SK3*; are expressed in the central nervous system (Kohler *et al.* 1996; Ishii *et al.* 1997; Joiner *et al.* 1997). *In situ* hybridization has revealed very high levels of SK3 but undetectable levels of SK1 and SK2 gene transcripts in SON (Stocker & Pedarzani, 2000), in correspondence with immunochemical staining for the SK3 subunit (Greffrath *et al.* 1998). Therefore, the mAHP in MNCs may be attributable specifically to the expression of SK3 channels.

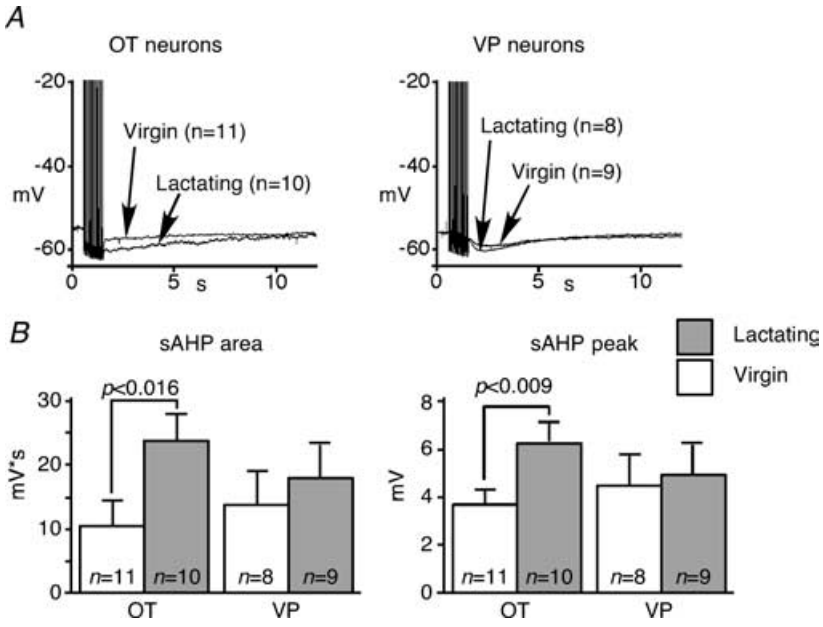

Figure 6. The sAHP increases during lactation
A, sAHP isolated by Cs^+ and apamin in OT and VP neurons. The traces are averaged among all cells. *B*, the peak and area of sAHP increased significantly in response to lactation among OT neurons, but not VP neurons. Error bars show S.E.M.

The present study demonstrated that the current density of the apamin-sensitive I_{mAHP} in OT neurons was specifically enhanced during lactation, and this probably accounts for the largest part of the increased AHP we observed in this study and previous investigations using sharp electrodes (Stern & Armstrong, 1996; Teruyama & Armstrong, 2002*a*). Moreover, this change appeared to be accomplished without apparent correlation with the cytoplasmic Ca^{2+} transient and the whole-cell Ca^{2+} currents (see below), and without a change in either the decay of the mAHP or I_{mAHP}. The latter results differ from our sharp electrode studies however, where we found an accelerated AHP decay during lactation. In the present study we blocked the time-overlapping DAP with Cs^{+} (Ghamari-Langroudi & Bourque, 1998), and isolated the mAHP with apamin. Since the DAP incidence is increased during lactation (Stern & Armstrong, 1996; Teruyama & Armstrong, 2002*a*), we suggest our previous results are probably the result of a combination of: (1) not isolating mAHP and sAHPs; and (2) competition of overlapping

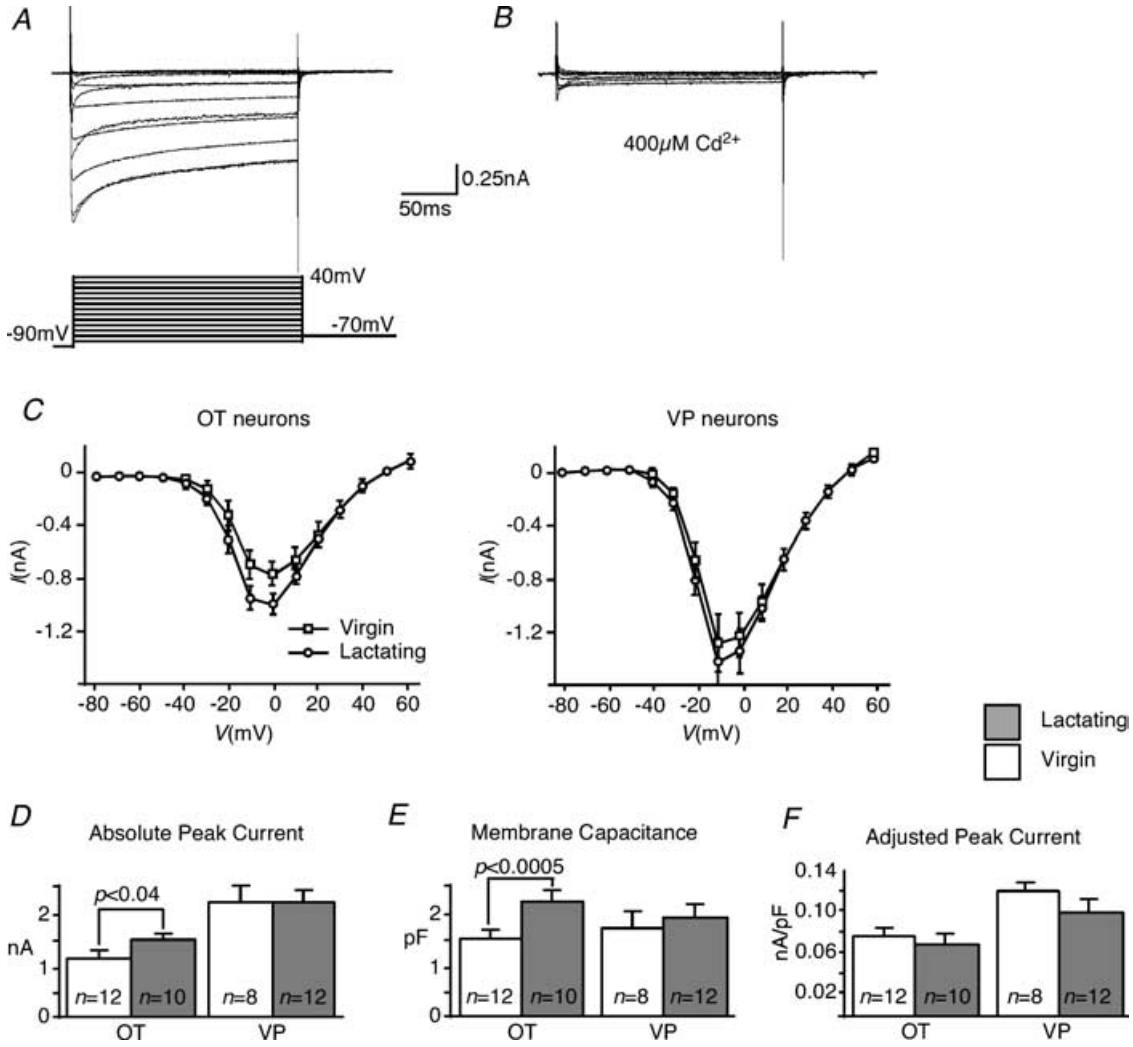

Figure 7. Whole-cell Ca^{2+} currents in the SON
A, an example of inward currents evoked by 200 ms steps with a good space-clamp control. The traces show currents generated by 200 ms steps from −90 mV to 40 mV in 10 mV increments. The peak current occurred between −10 and 0 mV. *B*, the inward currents evoked by 200 ms steps were completely blocked by 400 μM Cd^{2+}. Changes in whole cell Ca^{2+} current during lactation. *C*, *I–V* relationship of OT and VP neurons. The current values were obtained at the end of 200 ms square pulses. Peak current was between −10 and 0 mV. Apparent reversal potential was about +50 mV. Peak current values in OT neurons obtained from lactating rats were significantly larger at between −20 and 0 mV than those from virgin rats ($P < 0.05$). *D*, absolute peak and sustained (not shown) Ca^{2+} current increased significantly in OT neurons, but not VP neurons during lactation. *E*, the cell membrane capacitance increased significantly in OT neurons, not in VP neurons in response to lactation. *F*, peak Ca^{2+} current adjusted by whole-cell capacitance. When adjusted for whole-cell capacitance, the current density did not change in OT neurons during lactation. Error bars show S.E.M.

DAPs and AHPs. Although we cannot be sure of the precise mechanism, the most parsimonious explanation of the enhanced current density of I_{mAHP} is that SK3 channel density is upregulated during lactation. This would serve to strongly gate firing rate during the brief and explosive milk-ejection bursts of OT neurons.

Interestingly, it has been reported recently that the rat *SK3* gene is transcriptionally regulated by oestrogen, mediated by oestrogen receptor α (Jacobson *et al.* 2003). During pregnancy in rats, serum oestradiol concentration gradually increases from day 10 of gestation, and progressively rises in the last few days, while progesterone declines significantly between days 20 and 22 of pregnancy, reaching basal levels by parturition (Bridges, 1984). This increase in progesterone and oestradiol during pregnancy followed by the fall of progesterone prior to birth is known to be critical for ability of intracerebroventricular administration of OT to induce the milk ejection reflex (Housham & Ingram, 1995; Jiang & Wakerley, 1995). These imply a genomic modulation of the intrinsic properties of OT neurons. Previously, long-term (requiring at least 2 days) manipulation of oestradiol levels (castration with replacement treatments) was found to excite OT neurons from the PVN (Akaishi & Sakuma, 1985). These data suggest that oestrogen may have the ability to modulate I_{mAHP} or other ionic currents of OT

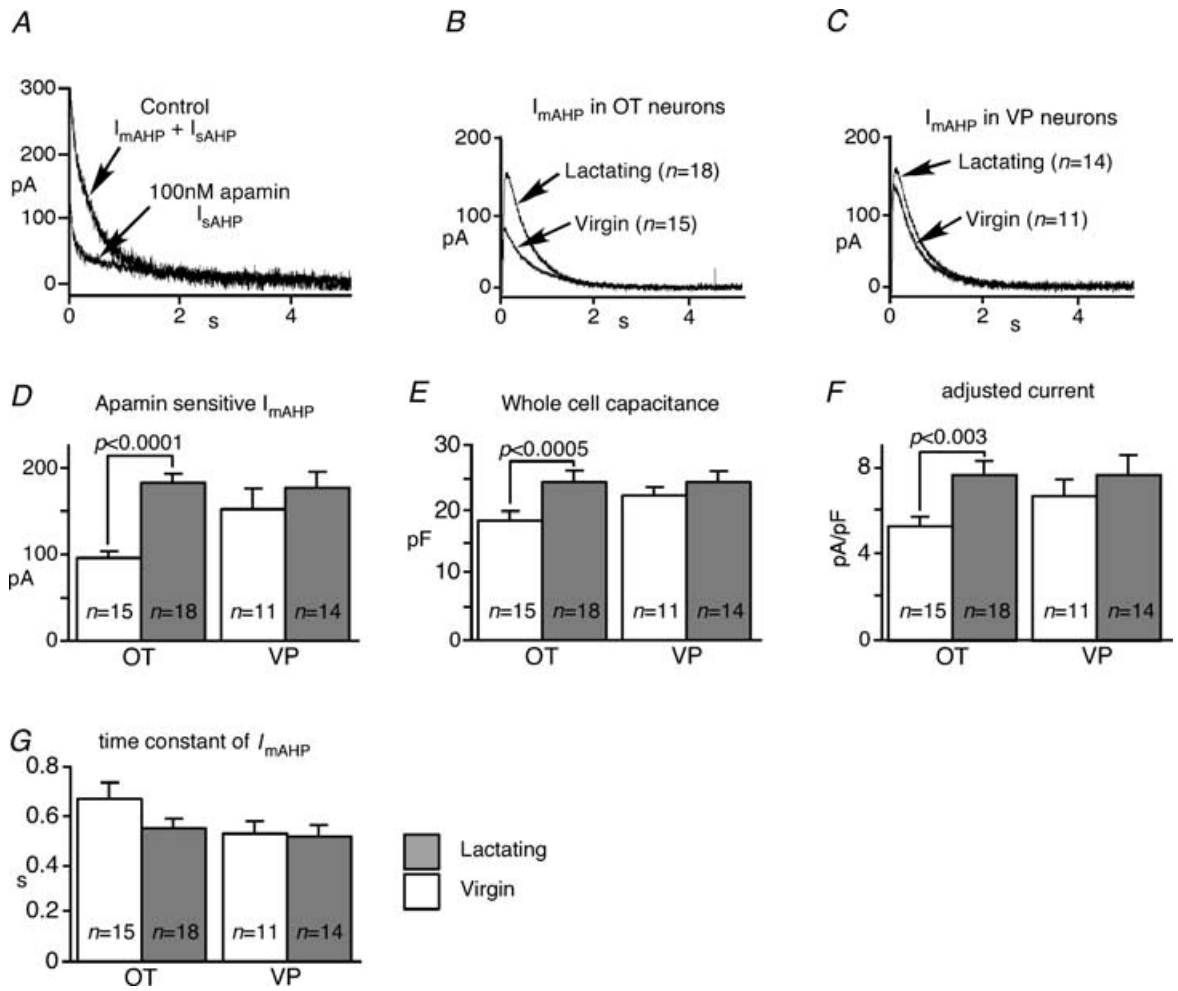

Figure 8. The apamin-sensitive I_{mAHP} increases during lactation
A, I_{AHP}. Outward tail currents evoked by 200 ms square pulse. The currents were well fitted by a double exponential curve indicating the presence of I_{mAHP} and I_{sAHP}. Application of 100 nM apamin blocked the I_{mAHP} so that I_{sAHP} is isolated. The apamin-sensitive I_{mAHP} was isolated by mathematical subtraction in OT (*B*) and in VP (*C*) neurons from lactating and virgin rats. *D*, the averaged peak amplitude of the apamin-sensitive I_{mAHP} in OT neurons was larger during lactation, but not in VP neurons. *E*, the cell membrane capacitance also increased significantly during lactation in OT neurons indicating hypertrophy, but not in VP neurons. F, The I_{mAHP} density was also increased significantly only in OT neurons, but not in VP neurons, during lactation, when the peak amplitudes of I_{mAHP} were adjusted for the cell membrane capacitance. *G*, the decay time constant of the I_{mAHP} in OT and VP neurons did not change significantly during lactation.

neurons through genomic actions. Although OT neurons in the rat SON are thought to lack the nuclear oestrogen receptor ER-α (Burbach *et al.* 1990; Simonian & Herbison, 1997), the presence of the nuclear receptor ER-β has been found (Shughrue *et al.* 1996; Li *et al.* 1997). However, the role of the ER-β in the SON is undetermined.

sAHP

In other neurons, particularly hippocampal and cortical pyramidal neurons, a Ca^{2+}-dependent sAHP has been intensely studied without any conclusion about the precise underlying channel. In general, sAHPs can be modulated by neurotransmitters such as noradrenaline and acetylcholine (ACh), have slow activation and decay kinetics, and are highly temperature sensitive (Sah & Faber, 2002). These factors have led to the suggestion that sAHP channels may not be directly gated by Ca^{2+} but rather work through a Ca^{2+}-dependent intermediary. In the SON, muscarinic receptor activation inhibits a sAHP in phasic (putative VP) neurons (Ghamari-Langroudi & Bourque, 2004). It is unknown whether the sAHP of OT neurons is also modulated by muscarine, but if so, we might expect a more important role for ACh during lactation. Intraventricular injections of muscarinic agonists or ACh are largely excitatory to OT release, and there is some evidence of these receptors on OT neurons (Richard et al. 1988; Crowley & Armstrong, 1992). Interestingly, the shape of the sAHPs differed between OT and VP neurons. In VP neurons, the sAHP was consistently slow to activate, peaking well after the end of the spike train, similar to the sAHPs of Ghamari-Langroudi & Bourque (2004), whereas in OT neurons the sAHP peaked earlier. Although the amplitude of sAHP in OT neurons is larger during lactation, only a relatively small change in whole-cell I_{sAHP} was observed, with no change in current density or decay. Therefore, the enhanced sAHP during lactation is probably not linked to changes in channel density, but perhaps in the relationship of the channels with Ca^{2+} or second messengers that may be involved in linking Ca^{2+} with sAHPs.

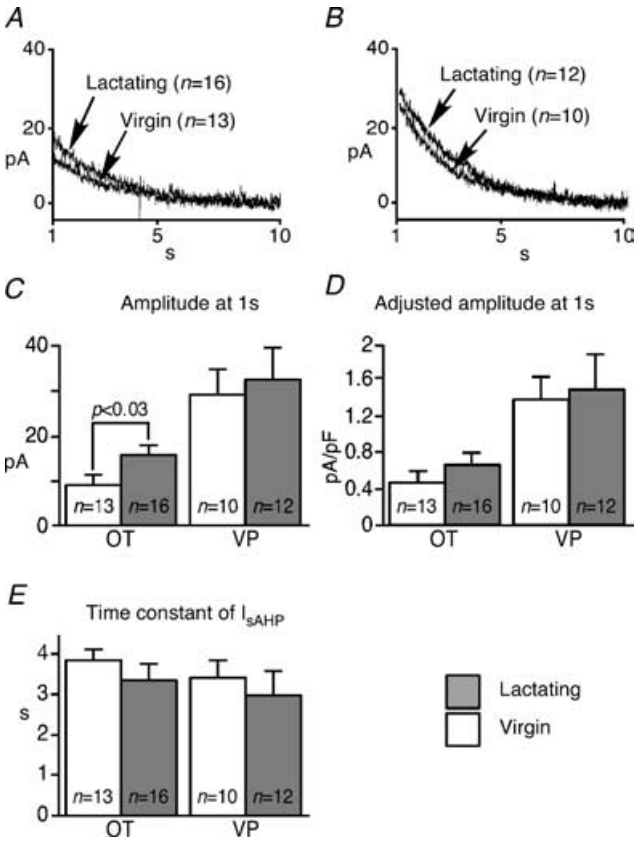

Figure 9. I_{sAHP} increases during lactation
The tail-current underlying the sAHP was observed after the application of Cs^+ and apamin in OT neurons (*A*) and VP neurons (*B*). The I_{sAHP} was well fitted by a single exponential curve. To avoid contaminating the data with the I_{fAHP}, all fits to I_{sAHP} decay began at 1 s after the end of square pulse where its amplitude was measured as an index of I_{sAHP} amplitude. *C*, the amplitude of I_{sAHP} increased in OT neurons during lactation, but not in VP neurons. *D*, when adjusted for whole-cell capacitance, current density of the I_{sAHP} did not change. *E*, the time constant did not change in response to lactation in either cell type. Error bars show S.E.M.

The failure to find a change in I_{sAHP} decay suggests that the changes in integrated amplitude of the sAHP are mostly due to the change in the peak. Furthermore, the more complicated time course of the sAHP relative to the monoexponential decay of I_{sAHP} would argue that other membrane events come into play during the long time course of repolarization during a sAHP. One example of an interacting current could be the sustained outward rectifier (SOR), a potassium current we previously described in OT neurons as contributing to prolonged spike frequency adaptation, and which is slow to deactivate (Stern & Armstrong, 1995).

Ca^{2+} current and $[Ca^{2+}]_i$

Since our previous studies (Stern & Armstrong, 1996; Teruyama & Armstrong, 2002*a*) had suggested a common feature of AHP and DAP plasticity might be their Ca^{2+} dependence, we tested whether AHP plasticity was related to changes in the whole-cell Ca^{2+} current or in $[Ca^{2+}]_i$. Although whole-cell Ca^{2+} current did increase coincident with the somatic hypertrophy of OT neurons during lactation observed previously (Russell, 1980; Theodosis & Poulain, 1993; Brussaard et al. 1999), current density was not increased. Neither did the peak Ca^{2+} transient ($\Delta F/F$). If the surface area of OT neurons increased and the Ca^{2+} current density remained constant, then, one can assume that bulk $[Ca^{2+}]_i$ should decrease due to the change in the surface to volume ratio. One explanation for this discrepancy could be increased Ca^{2+} release from

Ca^{2+}-dependent intracellular stores (Dayanithi et al. 2000) during lactation. Second, the cytoplasmic volume available for immediate Ca^{2+} diffusion might not change much, due to the significantly expanded endoplasmic reticulum observed during lactation (Kalimo, 1975).

We also cannot rule out a specific change in the density of a particular Ca^{2+} channel type at the expense of another. Several high-voltage-activated (HVA) Ca^{2+} channel types (L-, N-, P-, and Q-type channels) have been described in MNCs from the SON on the basis of pharmacology (Fisher & Bourque, 1996; Foehring & Armstrong, 1996; Joux et al. 2001), and specific types of voltage-gated Ca^{2+} channels can selectively activate different types of Ca^{2+}-activated K^+ channel. In hippocampal neurons, the source of calcium for SK channel activation was found to be L-type calcium channels, as Ca^{2+} influxes from L-type channels activate SK channels only, without activating large conductance BK channels (Marrion & Tavalin, 1998), whereas in neocortical pyramidal cells, mAHPs are coupled more to P-type channels, and several subtypes contribute to the sAHP (Pineda et al. 1998). A recent preliminary report suggests that during dehydration, L-channel density is increased selectively at the expense of other channel types in SON neurons, and the whole-cell Ca^{2+} current is unchanged (Star & Fisher, 2004).

Another caution is that AHPs could derive more from distal dendrites, and we have largely omitted sampling in the Ca^{2+} current studies from these areas. Some spatial differences have been noted for certain Ca^{2+} channel subtypes in SON neurons (Joux et al. 2001). Yet AHPs are large and common in slices, where dendrites often would be truncated; thus Ca^{2+} from distal dendrites would seem unlikely to contribute much to the AHPs we observed. Although relatively short compared to some neuronal types, SON dendrites take tortuous courses in the slice and we were not able to consistently sample them in this study. Thus it remains possible that even proximal dendritic Ca^{2+} channels and/or handling might differ during lactation, and this is something we intend to explore further.

Recently, an enhanced integrated somatic Ca^{2+} current at a single test pulse of 0 mV was reported in dissociated SON neurons during lactation, and in this case, changes were attributed to an increased Ca^{2+} flux per unit membrane (de Kock et al. 2003). However, the peptide type of these neurons was not identified, the profile of the current recorded is more transient than those we observed at the same step size, and finally, the internal pipette solution in this study differed from ours. These differences make precise comparisons difficult.

Even though we did observe a faster decay in the slow Ca^{2+} transient during lactation, this was evident in both OT and VP neurons, and the latter showed no AHP changes. We can only speculate that some aspect of lactation, whether it is through buffers or morphology, affects Ca^{2+} handling in both cell types. According to theoretical models, the initial phase of the time course of the bulk Ca^{2+} clearance is dominated by buffer systems, whereas the extrusion by the membrane pump becomes the main determinant of the slower time course (Sala & Hernandez-Cruz, 1990; Nowycky & Pinter, 1993). In our present study, some neurons revealed two time constants in the decay of the Ca^{2+} transients, as previously reported (Roper *et al.* 2003). Unfortunately, with the 20 spike/20 Hz protocol, not enough neurons in each group expressed the faster component to allow statistical comparison.

Unlike the DAP in these neurons (Roper *et al.* 2003), we did not find a strong temporal relationship between either the mAHP or the sAHP, and Ca^{2+} decay. The time course and amplitude of SK-mediated K^+ currents (I_{mAHP}) vary depending on the dynamics of cytoplasmic free Ca^{2+}, the location of SK channels relative to Ca^{2+} sources, and the intrinsic gating properties of the SK channels (Sah, 1996; Marrion & Tavalin, 1998). SK channels are constitutively bound to calmodulin (CaM) at its intracellular C terminus, and calmodulin serves as the Ca^{2+} sensor (Maylie *et al.* 2004). The binding of Ca^{2+} to CaM induces conformational alterations that are transduced to the CaM-binding domain and trigger opening of the channel pore (Maylie *et al.* 2004). Deactivation of channels occurs upon dissociation of Ca^{2+} from CaM (Maylie *et al.* 2004). Despite its strong Ca^{2+} dependence, and the fact that the peak Ca^{2+} transients observed were well within the affinity of Ca^{2+} for the calmodulin in SK channels (Xia *et al.* 1998; Roper *et al.* 2003), our results demonstrated that bulk somatic Ca^{2+} changes probably do not reflect the concentrations acting on the sensors that operate either AHP. In fact, the time course of the sAHP did not change despite the time course of the Ca^{2+} transient being faster with the low affinity fura-6f than with fura-2 in the cortical pyramidal cell (Abel *et al.* 2004). Our previous modelling study suggests that dissociation in the time courses is consistent with strong Ca^{2+} compartmentalization within the cell (Roper *et al.* 2003).

A few studies (Li *et al.* 1995; Li & Hatton, 1996; Voisin *et al.* 1996) have shown that Ca^{2+} buffering by Ca^{2+}-binding proteins plays an important role in regulation of firing pattern in MNCs of SON. A majority of OT neurons in rats express the Ca^{2+}-binding proteins calbindin D28k and calretinin, whereas only a small population of VP neurons expressed these proteins (Arai *et al.* 1999). Since calbindin D28k and calretinin have been shown previously to contribute to calcium homeostasis in other cell types (Chard *et al.* 1993), OT neurons may have a different Ca^{2+}-buffering capacity than VP neurons. The presence of these buffers may keep $[Ca^{2+}]_i$ at a level that optimizes the afterpotentials required to achieve the physiological demands. Indeed, Li & Hatton (1996) determined that DAPs, and phasic bursting, could be unveiled in putative OT neurons upon intracellular dialysis

of anticalbindin D28k, immunoneutralizing calbindin, and thus, reducing intrinsic Ca^{2+}-buffering capacity.

There is substantial somato-dendritic release of OT during the milk ejection reflex (Moos & Richard, 1989; Neumann *et al.* 1993), and a majority of OT neurons respond to OT with a rise in intracellular Ca^{2+} concentration (Lambert *et al.* 1994). This increase in intracellular Ca^{2+} is mediated by specific OT receptors and results from release of Ca^{2+} from internal stores, not high-voltage gated channels (Lambert *et al.* 1994). Thus, another aspect to consider is whether intracellular Ca^{2+} stores, and their modulation by the binding of locally released OT to autoreceptors, are involved in the enhanced DAP and AHP in OT neurons during lactation.

In fact, in the dorsal motor nucleus of the vagus, Ca^{2+} influx has been demonstrated to directly gate apamin-sensitive Ca^{2+}-dependent K^+ channels, while activating Ca^{2+} release from intracellular stores activates an apamin-insensitive sAHP (Sah & McLachlan, 1991). The generation of the DAP in presumptive VP neurons is reduced by blockade and depletion of Ca^{2+} release from internal stores, and amplified by enhancement of intracellular Ca^{2+} release (Li & Hatton, 1997). Moreover, our data on Ca^{2+} transients would argue this release would be targeted specifically to domains not reflected in somatic changes in $[Ca^{2+}]_i$. Thus future studies attempting to link $[Ca^{2+}]_i$ and afterpotentials in MNCs will require more precise knowledge of the morphological location of AHP channels and the Ca^{2+} compartment relevant to their activation.

References

Abel HJ, Lee JC, Callaway JC & Foehring RC (2004). Relationships between intracellular calcium and afterhyperpolarizations in neocortical pyramidal neurons. *J Neurophysiol* **91**, 324–335.

Akaishi T & Sakuma Y (1985). Estrogen excites oxytocinergic, but not vasopressinergic cells in the paraventricular nucleus of female rat hypothalamus. *Brain Res* **335**, 302–305.

Andrew RD & Dudek FE (1984). Intrinsic inhibition in magnocellular neuroendocrine cells of rat hypothalamus. *J Physiol* **353**, 171–185.

Arai R, Jacobowitz DM & Hida T (1999). Calbindin D28k and calretinin in oxytocin and vasopressin neurons of the rat supraoptic nucleus. A triple-labeling immunofluorescence study. *Cell Tissue Res* **298**, 11–19.

Armstrong WE, Smith BN & Tian M (1994). Electrophysiological characteristics of immunochemically identified rat oxytocin and vasopressin neurones in vitro. *J Physiol* **475**, 115–128.

Belin V, Moos F & Richard P (1984). Synchronization of oxytocin cells in the hypothalamic paraventricular and supraoptic nuclei in suckled rats: direct proof with paired extracellular recordings. *Exp Brain Res* **57**, 201–203.

Bicknell RJ (1988). Optimizing release from peptide hormone secretory nerve terminals. *J Exp Biol* **139**, 51–65.

Bond CT, Maylie J & Adelman JP (1999). Small-conductance calcium-activated potassium channels. *Ann N Y Acad Sci* **868**, 370–378.

Bourque CW (1988). Transient calcium-dependent potassium current in magnocellular neurosecretory cells of the rat supraoptic nucleus. *J Physiol* **397**, 331–347.

Bourque CW & Brown DA (1987). Apamin and d-tubocurarine block the afterhyperpolarization of rat supraoptic neurosecretory neurons. *Neurosci Lett* **82**, 185–190.

Bourque CW, Randle JC & Renaud LP (1985). Calcium-dependent potassium conductance in rat supraoptic nucleus neurosecretory neurons. *J Neurophysiol* **54**, 1375–1382.

Bridges RS (1984). A quantitative analysis of the roles of dosage, sequence, and duration of estradiol and progesterone exposure in the regulation of maternal behavior in the rat. *Endocrinology* **114**, 930–940.

Brussaard AB, Devay P, Leyting-Vermeulen JL & Kits KS (1999). Changes in properties and neurosteroid regulation of GABAergic synapses in the supraoptic nucleus during the mammalian female reproductive cycle. *J Physiol* **516**, 513–524.

Burbach JPH, Adan RAH, van-Tol HHM, Verbeeck MAE, Axelson JF, Leeuwen FWV, Beekman JM & Ab G (1990). Regulation of the rat oxytocin gene by estradiol. *J Neuroendocrinol* **2**, 633–639.

Chard PS, Bleakman D, Christakos S & Fullmer CS & Miller RJ (1993). Calcium buffering properties of calbindin D28k and parvalbumin in rat sensory neurones. *J Physiol* **472**, 341–357.

Crowley WR & Armstrong WE (1992). Neurochemical regulation of oxytocin secretion in lactation. *Endocr Rev* **13**, 33–65.

Dayanithi G, Sabatier N & Widmer H (2000). Intracellular calcium signalling in magnocellular neurones of the rat supraoptic nucleus: understanding the autoregulatory mechanisms. *Exp Physiol*, **85**, 75S–84S.

de Kock CP, Wierda KD, Bosman LW, Min R, Koksma JJ, Mansvelder HD, Verhage M & Brussaard AB (2003). Somatodendritic secretion in oxytocin neurons is upregulated during the female reproductive cycle. *J Neurosci* **23**, 2726–2734.

Dopico AM, Widmer H, Wang G, Lemos JR & Treistman SN (1999). Rat supraoptic magnocellular neurones show distinct large conductance, Ca^{2+}-activated K^+ channel subtypes in cell bodies versus nerve endings. *J Physiol* **519**, 101–114.

El Majdoubi M, Poulain DA & Theodosis DT (1996). The glutamatergic innervation of oxytocin- and vasopressin-secreting neurons in the rat supraoptic nucleus and its contribution to lactation- induced synaptic plasticity. *Eur J Neurosci* **8**, 1377–1389.

Fisher TE & Bourque CW (1996). Calcium-channel subtypes in the somata and axon terminals of magnocellular neurosecretory cells. *Trends Neurosci* **19**, 440–444.

Foehring RC & Armstrong WE (1996). Pharmacological dissection of high-voltage-activated $Ca2^+$ current types in acutely dissociated rat supraoptic magnocellular neurons. *J Neurophysiol* **76**, 977–983.

Ghamari-Langroudi M & Bourque CW (1998). Caesium blocks depolarizing after-potentials and phasic firing in rat supraoptic neurones. *J Physiol* **510**, 165–175.

Ghamari-Langroudi M & Bourque CW (2004). Muscarinic receptor modulation of slow afterhyperpolarization and phasic firing in rat supraoptic nucleus neurons. *J Neurosci* **24**, 7718–7726.

Gies U & Theodosis DT (1994). Synaptic plasticity in the rat supraoptic nucleus during lactation involves GABA innervation and oxytocin neurons: a quantitative immunocytochemical analysis. *J Neurosci* **14**, 2861–2869.

Greffrath W, Martin E, Reuss S & Boehmer G (1998). Components of after-hyperpolarization in magnocellular neurones of the rat supraoptic nucleus in vitro. *J Physiol* **513**, 493–506.

Hatton GI (1990). Emerging concepts of structure-function dynamics in adult brain: the hypothalamo-neurohypophysial system. *Prog Neurobiol* **34**, 437–504.

Housham SJ & Ingram CD (1995). Appearance of the facilitatory action of central oxytocin on milk- ejection. Independence from peri-partum steroidal changes. *Adv Exp Med Biol* **395**, 200–202.

Ishii TM, Maylie J & Adelman JP (1997). Determinants of apamin and d-tubocurarine block in SK potassium channels. *J Biol Chem* **272**, 23195–23200.

Jacobson D, Pribnow D, Herson PS, Maylie J & Adelman JP (2003). Determinants contributing to estrogen-regulated expression of SK3. *Biochem Biophys Res Commun* **303**, 660–668.

Jiang QB & Wakerley JB (1995). Analysis of bursting responses of oxytocin neurones in the rat in late pregnancy, lactation and after weaning. *J Physiol* **486**, 237–248.

Joiner WJ, Wang LY, Tang MD & Kaczmarek LK (1997). hSK4, a member of a novel subfamily of calcium-activated potassium channels. *Proc Natl Acad Sci U S A* **94**, 11013–11018.

Joux N, Chevaleyre V, Alonso G, Boissin-Agasse L, Moos FC, Desarmenien MG & Hussy N (2001). High voltage-activated Ca^{2+} currents in rat supraoptic neurones: biophysical properties and expression of the various channel alpha1 subunits. *J Neuroendocrinol* **13**, 638–649.

Kalimo H (1975). Ultrastructural studies on the hypothalamic neurosecretory neurons of the rat. III. Paraventricular and supraoptic neurons during lactation and dehydration. *Cell Tissue Res* **163**, 151–168.

Kirkpatrick K & Bourque CW (1996). Activity dependence and functional role of the apamin-sensitive K^+ current in rat supraoptic neurones in vitro. *J Physiol* **494**, 389–398.

Kohler M, Hirschberg B, Bond CT, Kinzie JM, Marrion NV, Maylie J & Adelman JP (1996). Small-conductance, calcium-activated potassium channels from mammalian brain. *Science* **273**, 1709–1714.

Lambert RC, Dayanithi G, Moos FC & Richard P (1994). A rise in the intracellular Ca^{2+} concentration of isolated rat supraoptic cells in response to oxytocin. *J Physiol* **478**, 275–287.

Lasser-Ross N, Miyakawa H, Lev-Ram V, Young SR & Ross WN (1991). High time resolution fluorescence imaging with a CCD camera. *J Neurosci Meth* **36**, 253–261.

Lev-Ram V, Miyakawa H, Lasser-Ross N & Ross WN (1992). Calcium transients in cerebellar Purkinje neurons evoked by intracell stimulation. *J Neurophysiol* **68**, 1167–1177.

Li Z, Decavel C & Hatton GI (1995). Calbindin-D28k: role in determining intrinsically generated firing patterns in rat supraoptic neurones. *J Physiol* **488**, 601–608.

Li Z & Hatton GI (1996). Oscillatory bursting of phasically firing rat supraoptic neurones in low-$Ca2^+$ medium: Na^+ influx, cytosolic Ca^{2+} and gap junctions. *J Physiol* **496**, 379–394.

Li Z & Hatton GI (1997). Reduced outward K^+ conductances generate depolarizing after-potentials in rat supraoptic nucleus neurones. *J Physiol* **505**, 95–106.

Li X, Schwartz PE & Rissman EF (1997). Distribution of estrogen receptor-beta-like immunoreactivity in rat forebrain. *Neuroendocrinology* **66**, 63–67.

Marrion NV & Tavalin SJ (1998). Selective activation of Ca^{2+}-activated K^+ channels by co-localized Ca^{2+} channels in hippocampal neurons. *Nature* **395**, 900–905.

Maylie J, Bond CT, Herson PS, Lee WS & Adelman JP (2004). Small conductance Ca^{2+}-activated K^+ channels and calmodulin. *J Physiol* **554**, 255–261.

Moos F & Richard P (1989). Paraventricular and supraoptic bursting oxytocin cells in rat are locally regulated by oxytocin and functionally related. *J Physiol* **408**, 1–18.

Neumann I, Russell JA & Landgraf R (1993). Oxytocin and vasopressin release within the supraoptic and paraventricular nuclei of pregnant, parturient and lactating rats: a microdialysis study. *Neuroscience* **53**, 65–75.

Nowycky MC & Pinter MJ (1993). Time courses of calcium and calcium-bound buffers following calcium influx in a model cell. *Biophys J* **64**, 77–91.

Pineda JC, Waters RS & Foehring RC (1998). Specificity in the interaction of HVA Ca^{2+} channel types with Ca^{2+}-dependent AHPs and firing behavior in neocortical pyramidal neurons. *J Neurophysiol* **79**, 2522–2534.

Poulain DA & Wakerley JB (1982). Electrophysiology of hypothalamic magnocellular neurones secreting oxytocin and vasopressin. *Neuroscience* **7**, 773–808.

Richard P, Moos F & Freund-Mercier M-J (1988). Bursting activity in oxytocin cells. CRC Press, Boca Raton.

Roper P, Callaway J, Shevchenko T & Teruyama R & Armstrong W (2003). AHP's, HAP's and DAP's: how potassium currents regulate the excitability of rat supraoptic neurones. *J Comput Neurosci* **15**, 367–389.

Russell JA (1980). Changes in nucleolar dry mass of the neurones of the paraventricular and supraoptic nuclei in the rat during pregnancy and lactation. *Cell Tiss Res* **208**, 313–325.

Sah P (1996). Ca^{2+}-activated K^+ currents in neurones: types, physiological roles and modulation. *Trends Neurosci* **19**, 150–154.

Sah P & Faber ES (2002). Channels underlying neuronal calcium-activated potassium currents. *Prog Neurobiol* **66**, 345–353.

Sah P & McLachlan EM (1991). Ca^{2+}-activated K^+ currents underlying the afterhyperpolarization in guinea pig vagal neurons: a role for Ca^{2+}-activated Ca^{2+} release. *Neuron* **7**, 257–264.

Sala F & Hernandez-Cruz A (1990). Calcium diffusion modeling in a spherical neuron. Relevance of buffering properties. *Biophys J* **57**, 313–324.

Shevchenko T, Teruyama R & Armstrong WE (2004). High-threshold, Kv3-like potassium currents in magnocellular neurosecretory neurons and their role in spike repolarization. *J Neurophysiol* **92**, 3043–3055.

Shughrue PJ, Komm B & Merchenthaler I (1996). The distribution of estrogen receptor-beta mRNA in the rat hypothalamus. *Steroids* **61**, 678–681.

Simonian SX & Herbison AE (1997). Differential expression of estrogen receptor alpha and beta immunoreactivity by oxytocin neurons of rat paraventricular nucleus. *J Neuroendocrinol* **9**, 803–806.

Star B & Fisher TE (2004). Dehydration increase 1-type ca^{2+} channel density in supraoptic nucleus. *Abstr Soc Neurosci* **422**, 7.

Stern JE & Armstrong WE (1995). Electrophysiological differences between oxytocin and vasopressin neurones recorded from female rats in vitro. *J Physiol* **488**, 701–708.

Stern JE & Armstrong WE (1996). Changes in the electrical properties of supraoptic nucleus oxytocin and vasopressin neurons during lactation. *J Neurosci* **16**, 4861–4871.

Stern JE & Armstrong WE (1997). Sustained outward rectification of oxytocinergic neurones in the rat supraoptic nucleus: ionic dependence and pharmacology. *J Physiol* **500**, 497–508.

Stern JE, Hestrin S & Armstrong WE (2000). Enhanced neurotransmitter release at glutamatergic synapses on oxytocin neurones during lactation in the rat. *J Physiol* **526**, 109–114.

Stocker M & Pedarzani P (2000). Differential distribution of three Ca^{2+}-activated K^+ channel subunits, SK1, SK2, and SK3, in the adult rat central nervous system. *Mol Cell Neurosci* **15**, 476–493.

Teruyama R & Armstrong W (2002*a*). Changes in the active membrane properties of rat supraoptic neurones during pregnancy and lactation. *J Neuroendocrinol* **14**, 933–944.

Teruyama R & Armstrong W (2002*b*). Changes in calcium currents in oxytocin neurons from rat supraoptic nucleus during lactation. *Abstr Soc Neurosci* **273**, 1.

Teruyama R & Armstrong W (2004). Changes in the calcium-activated k current in oxytocin neurons from rat supraoptic nucleus during lactation. *Abstr Soc Neurosci* **422**, 15.

Theodosis DT & Poulain DA (1993). Activity-dependent neuronal-glial and synaptic plasticity in the adult mammalian hypothalamus. *Neuroscience* **57**, 501–535.

Voisin DL, Fenelon VS & Herbison AE (1996). Calbindin-D28k mRNA expression in magnocellular hypothalamic neurons of female rats during parturition, lactation and following dehydration. *Brain Res Mol Brain Res* **42**, 279–286.

Xia XM, Fakler B, Rivard A, Wayman G, Johnson-Pais T, Keen JE, Ishii T, Hirschberg B, Bond CT, Lutsenko S, Maylie J & Adelman JP (1998). Mechanism of calcium gating in small-conductance calcium-activated potassium channels. *Nature* **395**, 503–507.

Acknowledgements

The authors thank Dr R.C. Foehring for reading earlier versions of this manuscript and Dr J.C. Callaway for providing software and technical advice in the calcium imaging.This research was supported by NIH grants NS23941 and HD41002 (WEA).